

Anisotropic magnetoresistance and anisotropic tunneling magnetoresistance in ferromagnetic metal break junctions

Kirill I. Bolotin, Ferdinand Kuehmann, and D. C. Ralph

Laboratory of Atomic and Solid State Physics, Cornell University, Ithaca, NY 14853 USA

(Dated: February 8, 2020)

We measure the resistance of perm alloy break junctions as a function of the angle between the saturated magnetization and the current, for both nanometer-scale metallic contacts and tunneling devices. In the tunneling regime, we find large changes in resistance that cannot be explained by the conventional theory of anisotropic magnetoresistance (AMR) in metals. For metallic contacts, we demonstrate that nanoscale samples can exhibit non-trivial evolution of the phase and magnitude of AMR with contact size, and deviations from the sinusoidal angular dependence found in bulk samples.

PACS numbers: 72.25.Ba; 73.63.Rt; 75.47.-m; 75.75.+a

The magnetoresistance properties of nanometer-scale magnetic devices can be quite different from those of larger samples. One aspect of this difference has been explored extensively in previous experiments – the resistance of magnetic domain walls created when the magnetic moment direction in one magnetic electrode is rotated relative to the moment in a second electrode [1, 2, 3, 4, 5, 6, 7, 8, 9]. Here we focus on a different aspect of the physics of magnetoresistance in nanoscale magnetic contacts – the anisotropic magnetoresistance (AMR) that arises when the magnetization throughout a device is rotated uniformly so as to change the angle between the direction of current flow and the magnetic moment. Our measurements are motivated by predictions of increased AMR for atomic-sized ballistic conductors [10] and indications of enhanced AMR in Ni contacts [8]. By making detailed studies of resistance as a function of field angle using mechanically-stable perm alloy contacts, we show directly that the size of the AMR signal can increase dramatically as the contact cross sections are narrowed to the nanometer-scale regime. Even more strikingly, we

find that point contacts which are completely broken, so as to enter the tunneling regime, also exhibit a tunneling anisotropic magnetoresistance effect (TAMR) as large as 25% when the magnetic-moment directions in the two contacts are rotated together while remaining parallel. The size of the effect is so large as to be comparable to the tunneling magnetoresistance (TMR) measured when the relative angle between the two moments changes. A qualitatively-similar effect was recently reported in a (GaMn)As magnetic semiconductor tunnel junction [11], but such effects have not been noted previously in junctions with ordinary transition-metal magnetic electrodes.

Our devices are fabricated on silicon substrates by aligned steps of electron beam lithography. We use thermal evaporation to deposit first 20-nm-thick gold contact pads and then 30-nm-thick magnetic perm alloy (Py

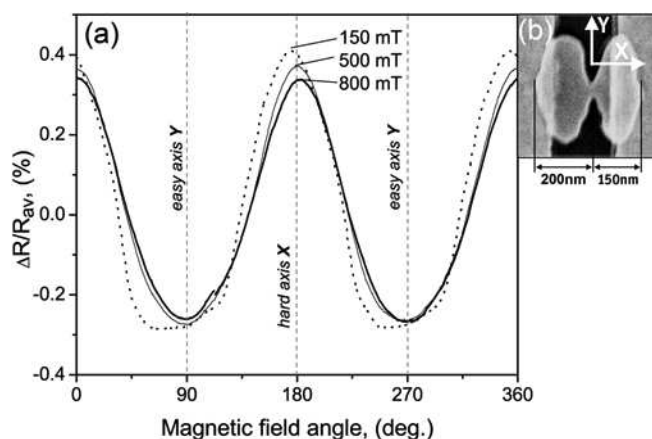


FIG. 1: (a) Change of resistance versus angle of applied magnetic field at different field magnitudes, illustrating bulk AMR for a sample with $R = 70 \, \Omega$ and a constriction size of $30 \times 100 \, \text{nm}^2$ (device A). (b) SEM micrograph of a typical device. The magnetic field angle is measured with respect to the x-axis for all samples.

$= \text{Ni}_{80}\text{Fe}_{20}$) point contacts [9]. Each point contact consists of two elongated electrodes which are connected by a 100-nm-wide bridge (Fig. 1(b)). We choose perm alloy because for iron concentrations around 20% its magnetostriction vanishes and its AMR is relatively large. The samples are measured while immersed in liquid helium. The magnetic field H is applied using a 3-coil vector magnet which is capable of applying up to 0.9 T in any direction and which can smoothly sweep the angle of the field at fixed magnitude. The device resistance R is measured by a resistance bridge with an accuracy better than 5 ppm; a total of 37 devices were studied.

Measurements are performed as follows: we first narrow the size of the bridge connecting the two magnetic electrodes by using actively controlled electromigration [12]. When the desired cross-section is reached (as determined by the sample's resistance) we stop the electromigration process and sweep the magnetic field while monitoring the resistance. Then the same procedure is re-

Electronic address: ralph@cornell.edu

peated to achieve smaller device cross-sections and larger resistances. As a result we can examine magnetic properties of each device as a function of the bridge size, down to the atomic scale and into the tunneling regime [9].

Magnetostriction and magnetostatic forces can affect the geometry of nanoscale junctions as the magnetic field is varied, and produce artifacts in the resistance, so it is crucial to take precautions to minimize these effects [5, 6, 7]. Point-contact devices formed by electromigration and measured at cryogenic temperatures have proven [8, 9] to be much more mechanically-stable than previous device structures measured at room temperature. This is because the devices are firmly attached to a non-magnetic substrate, with the only possibly-suspended part being the region affected by electromigration. In addition, our devices are fabricated from permalloy, a ferromagnetic alloy with a particularly small magnetostriction coefficient. Based on the electron microscopy images we determine that any possibly-suspended region in our devices (any thinned region showing less contrast) is less than 10 nm long. The contribution of magnetostriction to the resistance even in the most sensitive regime of tunneling can then be estimated using the Simmons formula [13]

$$\frac{R}{R_{av}}, \exp \frac{3 \lambda_s u^p}{2m_e} \sim 1; \quad (1)$$

where λ_s is the isotropic magnetostriction constant, u is the length of the suspended part of the junction, and

λ is the work function of the metal. Using realistic parameters ($\lambda_s < 10$ ppm, $u < 10$ nm, $\phi < 5$ eV) we estimate the maximum relative change in resistance due to magnetostriction to be less than 0.4%, i.e. more than 50 times smaller than the AMR we observe in our experiment, as discussed below. We also note that, for samples with resistances near that of a single quantum channel, magnetostriction is known to result in atomic rearrangements manifested as irreproducible jumps during the rotation of applied magnetic fields [5], a feature not seen in our data. Magnetostatic forces would give resistance changes of the opposite sign than we report below. Thus, unless the physics of magnetostriction is very different on the nanoscale than in bulk, neither magnetostriction nor magnetostatic forces can account for the AMR behavior we report.

To study the AMR, we rotate the magnetic field in the plane of the sample at fixed magnitude. The resistances of all devices before electromigration ($R \approx 70$ at 4.2 K) exhibit a small periodic dependence on the field direction ($\sim 1\%$, Fig. 1(a)). This is a signature of the bulk anisotropic magnetoresistance (AMR), which for a polycrystalline sample may be written [14]

$$R / R_{av} \sim \cos^2(\theta) \sim \frac{1}{2}; \quad (2)$$

where θ is the angle between the current and the magnetization M . The resistance of devices before electromigration is maximal for H applied in the x-direction

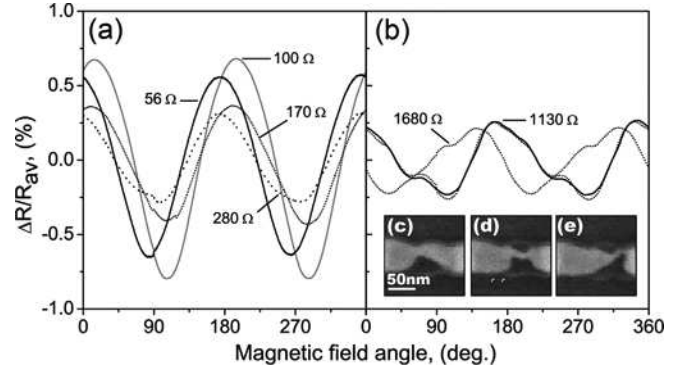


FIG. 2: (a) Evolution of anisotropic magnetoresistance in one device (device B) as its resistance is increased from 56 to 280 Ω , for a field magnitude of 800 mT. Both the amplitude and phase of the AMR can change. (b) The same device exhibits non-sinusoidal AMR at larger resistances: $R = 1130$ Ω (black line: $\mu_0 H_j = 800$ mT, gray line: $\mu_0 H_j = 500$ mT) and 1680 Ω ($\mu_0 H_j = 800$ mT). Insets (c), (d), (e): SEM pictures of a gold wire at different stages of controlled electromigration, showing changes in wire configuration that can occur.

(Fig. 1(b)), parallel to the current in the constriction. We measure the magnetic field angle relative to this direction.

Because the AMR depends on the orientation of the magnetization, it is crucial to ensure that the sample is magnetized uniformly and remains always saturated in the direction of the applied field. We estimated the distribution of magnetization within the sample using the OOMMF code [16]. Such modeling suggests that applying 800 mT effectively saturates the nanoscale magnetic electrodes for all directions in plane: the average M follows the magnetic field H to within 2° and the RMS fluctuation in the angle of magnetization across the sample is $\theta_M < 4^\circ$. To check this experimentally, we fit our 800 mT data to Eq. (2), and we found that the RMS deviation of the magnetization angle indicated by the fit was $\theta_M < 5^\circ$. We observe that the applied field becomes insufficient to fully saturate M below approximately 200 mT, at which point M departs from the field direction toward the easy axis of the sample. As a result, for low field strengths, the magnetoresistance as a function of field angle exhibits relatively flat-bottomed valleys for angles of H near the easy axis of the sample and sharpened peaks for H near the hard axis (Fig. 1(a), dotted curve).

We find that the AMR changes qualitatively and quantitatively as the cross section of a constriction is narrowed. While for large-width, low-resistance devices ($R < 200$ Ω) the AMR retains its $\cos^2(\theta)$ dependence on the field angle, both its phase and amplitude can change as the constriction becomes smaller (Fig. 2(a)). However, the amplitude of the AMR remains small ($R/R_{av} < 1.5\%$) for all devices with $R_{av} < 1$ k Ω , and does not depend consistently on the device's resistance. We can gain insight into the changing phases and amplitudes by ex-

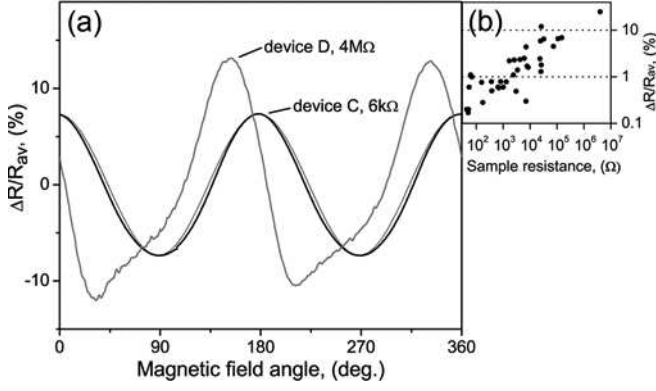


FIG. 3: (a) Device C: Anisotropic magnetoresistance of a 6 k device at a field magnitude of 800 mT, exhibiting 15% AMR. The AMR is well described by a $\cos^2(\theta)$ dependence (dotted line), without abrupt steps of the form predicted by ref. [10]. Device D: Tunneling device exhibiting 25% AMR. (b) AMR magnitude as a function of R for 7 devices studied in the tunneling regime.

analyzing electron-microscope images of gold test devices during different stages of electromigration (Fig. 2(b), insets { we used gold test devices rather than Py to optimize contrast during imaging). We see that electromigration often distorts the shape of the bridge connecting the electrodes as it is narrowed. As a result, in different segments of the bridge the current can flow at different angles with respect to the applied field. Assuming that Py bridges undergo the same types of conformational changes, different segments of the point contact could then contribute with different phases to the total AMR of the device. Since the angle-dependence of the AMR in every segment should remain sinusoidal, the total AMR of the bridge would still be sinusoidal as well, but it is natural that its amplitude and phase may undergo changes.

As the cross-section is reduced further, to the regime where the resistance is larger than several hundred Ω m, the angular dependence of the AMR for some samples (Fig. 2(b)) can become more complicated than the simple $\cos^2(\theta)$ form (Eq. (2)). By comparing sweeps at different field amplitudes we concluded that this was not due to a lack of saturation of the magnetization along the field direction at 800 mT (Fig. 2(b)). However, we suggest that this nonsinusoidal behavior should not be unexpected because Eq. (2) results from a rotational average that is strictly valid only for a polycrystalline sample [14]. As the cross section approaches the size of a crystalline grain, we expect that contributions to the AMR should be affected by the particular angular orientation of the atomic lattice in those grains. We note, however, that some samples retain near- $\cos^2(\theta)$ AMR dependence in all ranges of resistance.

We find that devices with resistances larger than 5 k generally exhibit much larger AMR. Figure 3 shows a 7 k device with an AMR of 14% (device C), more than

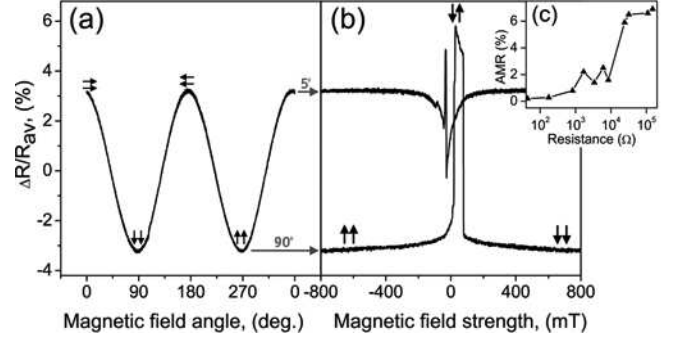


FIG. 4: (a) Tunneling anisotropic magnetoresistance as a function of magnetic field angle for a 100 k device (device E) at a fixed amplitude of 800 mT, sufficient to saturate the moments in both electrodes. (b) Change of resistance as a function of the magnetic field amplitude at two fixed angles of 5° and 95° for the same device. The resistance change in the vicinity of zero field (TMR) exceeds the magnitude of the TAMR, but the two effects are comparable. (c) AMR value as a function of device resistance for the same sample.

50 times the value for this device before electromigration. The angular dependence of the AMR for this sample remains $\cos^2(\theta)$ to a very good approximation. Even for samples in the tunneling regime ($R > 20$ k) we continue to measure large values of AMR (Fig. 4(a)), as large as 25% in a 2 M sample (Fig. 3(a), device D). This cannot result from the conventional AMR mechanism, which affects the metallic resistance through modifications of electron scattering, and which should therefore become negligible when the tunneling resistance dominates the metallic resistance of the electrodes. The dependence of the AMR on sample resistance in the tunneling regime is shown in Fig. 3(b).

It is interesting to compare the magnitude of this large tunneling anisotropic magnetoresistance (TAMR), measured by keeping the magnetic moments of the electrodes parallel while varying their angle, to the conventional tunneling magnetoresistance (TMR) measured by changing the relative angle of the moments in the two electrodes. We can measure TMR by sweeping the magnitude of the magnetic field at fixed angle; near zero field we observe changes in resistance associated with the reversal of the moment in one and then the other electrode (Fig. 4(b)). Comparison with Fig. 4(a) shows that the resistance change due to the TAMR effect is a large fraction of the TMR signal, so that the two effects must be considered together for accurate analyses of the total magnetoresistance. For example, the TAMR can be large enough to invalidate procedures which use the value of the magnetoresistance to evaluate the degree of tunneling polarization in a nanoscale contact.

We can characterize our experimental findings as follows: when the sample's conduction is primarily metallic we observe AMR signals in reasonable accord with ordinary bulk AMR. After tunneling begins to contribute a significant fraction of the transport signal ($R \gtrsim 5$ k),

we see a large enhancement of AMR which cannot be accounted for by either bulk AMR or standard TMR effects.

Two recent theoretical papers have analyzed AMR in atomic-sized contacts [10] and in the tunneling regime [15]. Velev et al. [10] predicted a large increase in AMR for atomic-sized ballistic conductors, when the current is carried via just a few quantum channels. They argued that changing the magnetization direction in such a system may "pinch on" and "pinch off" individual channels of conduction, leading to step-like increases and decreases in the conductance at angles of magnetization determined by the conductor's geometry. We note that none of our devices show such features, and in fact most of our largest AMR and TAMR signals exhibit to a very good accuracy a simple $\cos^2(\theta)$ angular dependence (Fig. 3(a) device C and Fig. 4(a)).

AMR in the tunneling regime was analyzed by Shick et al. [15]. They argued that the tunneling density of states (DOS) of nanoscale ferromagnets can be changed by varying the direction of \mathbf{M} . Based on relativistic band structure calculations they predicted large ($\sim 20\%$) anisotropy of the DOS for nanoscale CoPt devices, which would result in large TAMR values. They also found that the effect is sensitive to the detailed geometry of the contacts. This mechanism captures our observed increase in AMR in the tunneling regime and the variation

of AMR values between devices, and thus seems to agree well with our experiments. A related effect was measured recently in a magnetic semiconductor device [11], but to our knowledge our measurements are the first to show tunneling anisotropic magnetoresistance between metal electrodes.

In summary, we have measured the AMR for a metal ferromagnet as a function of its cross-section. We studied regimes from bulk-like ($100 \times 30 \text{ nm}^2$ cross sections) to atomic-scale point contacts and into the tunneling regime, and found a nontrivial evolution of the AMR. For low-resistance devices we observed that both the phase and magnitude of the effect could change as the cross-section is narrowed. We also observed a nonsinusoidal angular dependence of the AMR in some devices with narrowed constrictions. These effects appear to be consistent with the conventional AMR mechanism. In devices approaching the atomic scale and in tunneling regime we found a dramatic enhancement of AMR, to values as large as 25%. The effect is large enough that the resistance changes due to TAMR are comparable to the conventional tunneling magnetoresistance due to magnetization reversal in nanoscale junctions.

We thank Eric Smith for experimental help. This work was funded by the NSF (DMR-0244713 and through the use of the Cornell NanoScale Science & Technology Facility/NNIN) and by the ARO (DAAD19-01-1-0541).

-
- [1] P. M. Levy and S. F. Zhang, Phys. Rev. Lett. 79, 5110 (1997).
 - [2] N. Garcia, M. Munoz, and Y. W. Zhao, Phys. Rev. Lett. 82, 2923 (1999).
 - [3] S. Z. Hua and H. D. Chopra, Phys. Rev. B 67, 060401(R) (2003).
 - [4] M. Viret, S. Berger, M. Gabureac, F. Ott, D. Olligs, I. Petej, J. F. Gregg, C. Fernon, G. Francinet, and G. LeGoff, Phys. Rev. B 66, 220401(R) (2002).
 - [5] M. Gabureac, M. Viret, F. Ott, and C. Fernon, Phys. Rev. B 69, 100401(R) (2004).
 - [6] C. S. Yang, C. Zhang, J. Redepenning, and B. Doudin, Appl. Phys. Lett. 84, 2865 (2004).
 - [7] W. F. Egelho, L. Gan, H. Ettedgui, Y. Kadmon, C. J. Powell, P. J. Chen, A. J. Shapiro, R. D. McMichael, J. J. Mallett, T. P. Moat, et al., J. Magn. Magn. Mater. 287, 496 (2005).
 - [8] Z. K. Keane, L. H. Yu, and D. Natelson, cond-mat/0510094.
 - [9] K. I. Bobkin, F. Kuemmeth, A. N. Pasupathy, and D. C. Ralph, Nano Lett. 6, 123 (2006).
 - [10] J. Velev, R. F. Sabirianov, S. S. Jaswal, and E. Y. Tsymsbal, Phys. Rev. Lett. 94, 127203 (2005).
 - [11] C. Gould, C. Ruster, T. Jungwirth, E. G. Giris, G. M. Schott, R. Giraud, K. Brunner, G. Schmidt, and L. W. Molenkamp, Phys. Rev. Lett. 93, 117203 (2004).
 - [12] D. R. Strachan, D. E. Smith, D. E. Johnston, T. H. Park, M. J. Therien, D. A. Bonnell, and A. T. Johnson, Appl. Phys. Lett. 86, 043109 (2005).
 - [13] E. L. Wolf, Principles of Electron Tunneling Spectroscopy (Oxford University Press, New York, 1989).
 - [14] T. R. McGuire and R. I. Potter, IEEE Trans. on Magn. 11, 1018 (1975).
 - [15] A. B. Shick, F. Mica, J. Masek, and T. Jungwirth, Phys. Rev. B 73, 024418 (2006).
 - [16] OOMF is Object Oriented MicroMagnetic Framework, a micromagnetic simulation code freely available from NIST at <http://math.nist.gov/oommf/>